Trends in Immunology

CellPress

Review

T Cell Development by the Numbers

Andreas Krueger,[1,*] Natalia Ziętara,[2] and Marcin Łyszkiewicz[2]

T cells are continually generated in the thymus in a highly dynamic process comprising discrete steps of lineage commitment, T cell receptor (TCR) gene rearrangement, and selection. These steps are linked to distinct rates of proliferation, survival, and cell death, but a quantitative picture of T cell development is only beginning to emerge. Here we summarize recent technical advances, including genetic fate mapping, barcoding, and molecular timers, that have allowed the implementation of computational models to quantify developmental dynamics in the thymus. Coupling new techniques with mathematical models has recently resulted in the emergence of new paradigms in early hematopoiesis and might similarly open new perspectives on T cell development.

T Cell Development: A Model Process with Clinical Relevance

T cell development is a highly dynamic process and essentially continues throughout the life of an organism. In contrast to other hematologic cell lineages, T cells do not complete their development in the bone marrow (BM). Rather, BM-derived progenitor cells migrate to the thymus where cells complete lineage commitment, undergo somatic rearrangement of their TCR genes, and undergo selection to prevent the emergence of autoreactive cells (Box 1).

Production of naïve T cells declines with increasing age due to thymic involution. Although generally not a problem in healthy individuals, this decline is a major underlying problem early after hematopoietic stem cell (HSC) transplantation (HSCT). Preconditioning regimens eradicate the patient's immune system and only small numbers of T cells can be generated *de novo* in an involuted thymus. As a consequence, elderly patients especially suffer a prolonged phase of immunodeficiency after HSCT. Enhancing T cell regeneration or 'rejuvenating' the aging thymus is therefore paramount to improve the outcome of HSCT [1].

Understanding T cell development is not only a prerequisite for the development of therapeutic strategies. T cell development has also served as a model process fostering our understanding of cell fate determination through gene regulatory networks, extrinsic signals, and specialized tissue microenvironments [2]. Thus, in qualitative terms T cell development is extremely well characterized. T cells are generated from a minute pool of hematopoietic progenitor cells that has to expand drastically to generate a diverse range of selectable clones and then undergoes stringent selection and a productive output of only about 1% T cells compared with the overall number of thymocytes. Despite these variations in cell number across T cell development, a quantitative picture of this process is less well developed. Recently, substantial progress has been made in developing lineage fate-tracing techniques, molecular timers, cellular barcoding, and other sophisticated genetic reporters, all of which are increasingly accessible to quantitation and mathematical modeling. Such approaches have recently fundamentally changed current models of early hematopoiesis [3,4].

Here we summarize technical advances and their incorporation into mathematical models. We then go on to outline recent findings that allow us to draw a quantitative image of key stages of T cell development highlighting areas where quantitative information is still largely missing.

Trends

T cell development is serving as a model process for the study of fundamental questions of developmental biology.

Understanding T cell development, at both the qualitative and quantitative level, is critical for improving immune regeneration after hematopoietic stem cell transplantation.

Refined experimental tools, particularly lineage fate tracing, cellular barcoding, reporter gene technology, and molecular timers, have been critical for the development of computational models that are sufficiently accurate to generate new hypotheses.

Computational models have been pivotal in generating new paradigms of steady-state hematopoiesis, in quantitating thymus colonization, and in dissecting thymic selection processes.

[1]Institute of Molecular Medicine, Goethe University Frankfurt am Main, 60590 Frankfurt am Main, Germany
[2]Dr von Hauner Children's Hospital, Ludwig Maximilian University, 80337 Munich, Germany

*Correspondence: andreas.krueger@kgu.de (A. Krueger).

Box 1. Intrathymic T Cell Development

TSPs enter the thymus from the blood through large venules at the CMJ, which is located at the border of the cortex and the medulla. TSPs occupy approximately 160 niches localized in the cortex and eventually give rise to ETPs, the most-immature detectable thymocyte population. In response to chemokine gradients and interactions with thymic epithelial cells (TECs) and other stromal cells, they migrate to the outer cortex while continuously progressing through $CD4^{-}CD8^{-}$ DN stages. T lineage commitment is completed with expression of the transcription factor Bcl11b at the DN2 stage. Somatic rearrangements of the *Trb*, *Trg*, and *Trd* TCR gene loci are initiated at the DN2 stage and continue at the DN3 stage followed by β selection in the subcapsular region of the cortex. Cells with productive rearrangement of the *Trg* and *Trd* genes enter the γδT lineage. Cells with productive rearrangement of the *Trb* locus signal via the pre-TCR resulting in allelic exclusion, proliferation, and developmental progression towards the $CD4^{+}CD8^{+}$ DP stage. DP cells occupy most of the cortex (80% of all thymocytes) and start to rearrange their *Tra* locus encoding the TCRα chain. This rearrangement produces a 'complete' TCR and is followed by additional selection steps. These selection events eventually result in the elimination of 90% of all cells. Positive selection ensures the survival of cells expressing an αβTCR capable of recognizing peptide:MHC ligands. By contrast, negative selection results in clonal deletion of cells expressing a TCR recognizing self-antigens. Negative selection can occur simultaneously with positive selection in the thymic cortex, most likely leading to deletion of clones reactive to ubiquitously expressed self-antigens. Alternatively, positive selection induces migration to the thymic medulla where thymocytes are probed for recognition of tissue-specific self-antigens, again resulting in deletion or terminal maturation. Whether a thymocyte undergoes positive or negative selection is essentially determined by its TCR's affinity for antigen:MHC. A minimal TCR signal is required to prevent death by neglect. However, high-affinity TCR–antigen:MHC interaction results in clonal deletion or, in some cases, the development of thymic regulatory T cells or natural killer T cells. The latter process is termed agonist selection. Finally, mature SP T cells emigrate from the thymus via post-capillary venules in the medulla to establish the peripheral naïve T cell pool.

Prologue in the Bone Marrow

HSCs and their progeny in BM have long been a focus of quantitative biology. For instance, it has been of interest to quantitate the lifetime of individual HSCs as well as their progeny to determine quiescence and self-renewal or the number of progenitors required for successful BM transplantation. Unsurprisingly, these fundamental questions have sparked the development of progressively refined technologies capable of quantification by mathematical modeling. Classically, experiments to map the fate of distinct cell populations to derive quantitative data comprised labeling with nucleoside analogs such as BrdU and transplantation experiments using chromosomal or congenic marks [5,6]. Current state-of-the-art methods essentially reflect more refined versions of either approach or a combination of the two. In contrast to BrdU labeling, inducible molecular timers based on fluorescent proteins with a distinct half-life such as GFP-histone 2B fusion proteins can confer cell-type specificity permitting the application of more refined mathematical models [7]. Clonal tagging via retroviral barcoding vastly expands the number of traceable clones compared with transplantation of one or at best two congenically marked grafts [8–10]. These experiments were directly able to show that after transplantation low numbers of HSCs (in the range of tens), only some of which are simultaneously active, regenerate the hematopoietic system [8,9]. Furthermore, these studies revealed a certain lineage bias in multipotent progenitors (MPPs) and even HSCs [8,10]. Thus, a substantial number of barcoded lymphoid-primed MPPs (LMPPs) were restricted to one or two rather than all lineages suggesting that regulatory programs of lineage decisions are in place before clear phenotypic changes. Cellular barcoding permits the application of computational models to calculate the probability of lineage decisions [11]. However, retroviral barcoding has several technical and biological limitations. Technically, faithful discrimination of true barcodes and sequencing errors remains a challenge [12]. Even more importantly, *ex vivo* manipulation followed by transplantation constitutes one of the major disadvantages of viral barcoding. Ultimately, it cannot be excluded that bias is introduced during however limited *in vitro* culture. Recently, two studies suggested that steady-state hematopoiesis differs substantially from the transplantation scenario. Sun *et al.* developed a system relying on transient activation of a transposon [3]. Quasi-random integration of this transposon resulted in the generation of clonal tags *in situ* without prior manipulation *in vitro*. This study demonstrated that the number of progenitor clones contributing to hematopoiesis at steady state was substantially higher than on transplantation. In addition, analysis of overlaps of

clonal marks between precursors and progeny indicated that over long periods of time (1 year) steady-state hematopoiesis is sustained by MPPs or, in the case of granulocytes, even myeloid-restricted progenitors rather than classically defined long-term reconstituting HSCs. Despite these paradigm-changing findings, the study by Sun *et al.* suffered from the disadvantage that transposon activation occurred in multiple cell types simultaneously, including HSCs and more differentiated populations. As a consequence, cell fate and population dynamics could not be directly traced back to the HSC compartment. This limitation was recently overcome by Busch *et al.*, who generated a genetic fate-mapping model of long-term reconstituting (LT)-HSCs [4]. In this model an inducible variant of Cre recombinase was expressed specifically in LT-HSCs allowing stage-specific and temporally controlled irreversible pulse labeling by a reporter gene. Reporter-positive cells could subsequently be traced over time throughout the hematopoietic tree. Applying a mathematical model to this system allowed the authors to determine the number of active HSCs and the flux of progenitor cells through the hematopoietic tree, including the residence time and differentiation rates of progenitor cells within stem and progenitor cell populations. Surprisingly, approximately 30% of an estimated 17 000 HSCs contributed to hematopoiesis, a much higher frequency than predicted by transplantation experiments. Fundamental differences between transplantation and steady-state hematopoiesis were also evident in the highly variable degree of label retention after transplantation. The residence time of cells within short-term HSCs and MPPs was determined to be 330 and 70 days, respectively, providing quantitative confirmation of the conclusion that steady-state hematopoiesis is sustained independent of LT-HSCs for extended periods of time [3,4]. Moreover, a strong quantitative bias towards the myeloid lineage was observed at the myeloid versus lymphoid lineage branch point, consistent with a generally shorter lifespan of myeloid cells compared with lymphocytes and massive proliferation events during later stages of lymphocyte development. Findings from this study were extensively reviewed in [13]. Recently, the idea that steady-state hematopoiesis relies on non-LT-HSCs has been challenged based on the analysis of a novel genetic model of HSC-specific fate mapping [14]. While based on the same experimental strategy of inducible genetic fate mapping this model allowed a much higher degree of labeling of the LT-HSC population compared with the model developed by Busch *et al.* (~30% vs ~1%) [4]. Following label progression longitudinally in individual animals after efficient HSC marking revealed a substantial contribution of HSCs to adult hematopoiesis, with otherwise similar conclusions to Busch *et al.* [4,14]. This new study highlights a critical limitation of computational modeling in its complete reliance on the quality of the experiment to which the computational model is applied. A combination of HSC-specific fate mapping and *in situ* barcoding, which is currently being developed, might provide additional insight into quantitative aspects of lineage decisions that either method alone cannot achieve [15].

Journey from Blood to Thymus

Under physiologic conditions, T cell development depends on continual colonization of the thymus by BM-derived thymus-seeding progenitors (TSPs). Candidate TSPs comprise a heterogeneous mixture of MPPs, common lymphoid progenitors (CLPs), and CLP-like cells as well as already T lineage-committed progenitors. Their phenotype and differentiation potential have been extensively reviewed elsewhere [16,17].

The numbers of candidate TSPs circulating in peripheral blood are extremely small. Thus, blood from a mouse contains approximately 180 MPPs, 600 circulating T lineage-committed progenitors, and 180 CLPs [18–22]. It remains to be established whether progenitor numbers in peripheral blood are actively maintained through controlled release from BM or passively due to a lack of survival factors [23]. The residence time of HSCs and progenitors in circulation was estimated to be in the range of only 6 min, suggesting that peripheral blood does not constitute a conductive environment for BM-derived progenitors [24].

Transfer experiments relying on progenitor depletion rather than enrichment into non-manipulated recipients as well as genetic fate-mapping experiments indicate that TSPs comprise multiple populations [25–27]. A minimal phenotypic requirement for TSPs is expression of the surface markers CD27 and/or CD135. This phenotype includes both MPP subsets and CLP-like cells. On the molecular level, thymus colonization is controlled in a highly redundant manner. Thus, deficiency in individual chemokine receptors or P-selectin ligand results in only a modest defect in thymus seeding [28–31]. However, compound deletion of CC chemokine receptors CCR7 and CCR9 on TSPs virtually abrogated thymus colonization in non-conditioned hosts and led to concomitant paucity of early T lineage progenitors (ETPs), the most immature detectable population of thymocytes [28,32].

Quantitation of thymus colonization at steady state has been complicated by the heterogeneity of TSPs and their phenotypic dissimilarity with ETPs. Nevertheless, attempts to quantitate thymus colonization, mostly of irradiated hosts, have been made over several decades [33]. Such attempts were based on limiting dilution assays and/or transplantation of a mixture of two congenically or chromosomally distinct donor populations. The latter approach permitted an estimate of thymus colonization by assessing the variance within a binomial distribution [34]. These experiments suggested that the irradiated thymus is colonized by 10–200 cells per day. Direct cytometry-based detection of donor-derived cells in short-term assays resulted in the recovery of much higher cell numbers, suggesting that the thymus sustains only a fraction of the progenitor cells that migrate there for entry into the T lineage [35–37].

Recently, thymus colonization was reassessed using an approach that was accessible to mathematical simulation and at the same time circumvented problems of direct detection as well as accidental counting of cells not entering the T lineage. This approach, termed multicongenic fate mapping (Figure 1), essentially represented an extension of earlier transfer experiments of two congenically marked populations to up to 13 congenically different fractions [38]. Transplantation of mixtures with defined ratios followed by determination of the number of congenic tags missing in donor-derived thymocytes permitted the implementation of Monte Carlo simulation to determine the number of colonization events. The focus on counting missing tags was important, as the readout was reduced to a binary present/absent call rather than having to take into account intrathymic differentiation processes. Multicongenic fate mapping-based simulation showed that a non-irradiated wild-type thymus could be colonized by on average ten TSPs at a given time [38]. The same approach was employed to estimate the overall number of niches available for TSPs. To this end, mice deficient in CCR7 and CCR9 were used

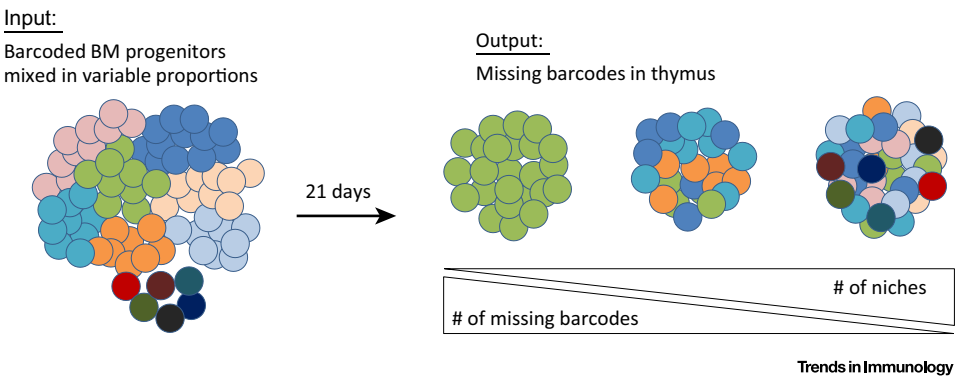

Figure 1. Congenic Barcoding Allows Quantification of the Number of Intrathymic Niches Supporting T Cell Development. Defined mixtures of congenically/fluorescently tagged bone marrow (BM)-derived progenitors are injected into non-irradiated hosts. After 21 days the number of missing tags is assessed in the thymus. A Monte Carlo simulation was used to quantify the number of intrathymic niches supporting T cell development based on this number of missing tags [38].

as recipients based on their near absence of ETPs while at the same time maintaining *bona fide* normal overall thymic cellularity. These experiments showed that the thymus contains approximately 160 niches for seeding by TSPs. Interestingly, conditioning through sublethal irradiation essentially liberated all available niches for colonization, implying that this type of conditioning is beneficial for T lineage regeneration despite inducing a certain degree of tissue damage. In these experiments application of mathematical models proved essential for two reasons. First, direct visualization of TSPs was impossible due to their elusive phenotype and low numbers, which bordered on the detection limit of flow cytometry. Second, a mathematical model permitted the design of a quantitative experiment with a clear binary (present or absent) readout.

It remains an open question how thymus colonization is regulated. Based on parabiosis experiments it has been proposed that thymic niches open periodically at 3–4-week intervals [39]. However, niche saturation through intrathymic transfer and sequential congenic fate-mapping experiments indicated a periodicity of 10–14 days; that is, an individual thymus acquires maximum receptivity for colonization every 10–14 days with a refractory period in between [38,40]. Interestingly, this period coincides with the average lifetime of an ETP as well as with the time of residence of transplanted thymocytes at the corticomedullary junction (CMJ), which constitutes the region of thymocyte entry [41,42]. These data suggest that the presence of ETPs near the CMJ might preclude TSPs from entry. Vascular endothelial cells that depend on lymphotoxin-β receptor signaling through crosstalk with thymocytes have recently been proposed to play a critical role in thymus colonization by TSPs [43,44] and it has been shown that ETPs receive signals through the c-kit receptor by membrane-bound stem cell factor (SCF) on such cells [45]. Thus, it is plausible that TSPs compete with intrathymic ETPs for the same source of SCF. It has also been proposed that more mature double-negative thymocytes (DN3s) rather than more immature populations provide negative feedback for thymus colonization [46]. However, DN3-mediated feedback was not observed in mice deficient in CCR7 and CCR9, highlighting the need for more refined models to study cellular and molecular feedback controlling thymus colonization [38].

Early Events: From 160 TSPs to 100 000 000 Double-Positive (DP) Thymocytes in 16–20 Days

The transition from approximately 160 TSPs to a readily detectable population of 20 000 to 30 000 ETPs constitutes a major black box in our understanding of early T cell development, which includes essentially all events before to definitive T lineage commitment. Although on the molecular level transcription factor hierarchies have been established that lead to the eventual commitment step reflected by expression of Bcl11b, it remains unclear how alternative lineage potential is efficiently repressed early on thymus seeding [17,47,48]. TSPs and ETPs combined have been estimated by transplantation of BM-derived progenitors to have an average lifetime of 9–12 days [42] during which they divide almost once per day. These data have recently been employed to generate a dynamical model of early T cell development to generate estimates for the residence time of cells within each thymocyte population and the cell cycle duration as well as probabilities of death or developmental progression [49]. In addition to providing a valuable set of quantitative data, this model was devised to address the question of whether commitment occurs randomly and independent of cell division within ETPs or whether it is more likely that commitment occurs only after a certain amount of proliferation has been completed. Modeling suggested that the latter scenario was more consistent with available data, highlighting the value of such approaches. Thus far, this model did not take into account that the source of ETPs is heterogeneous, comprising at least CLP and MPP subsets as well as possibly some other progenitor populations. It remains to be determined whether these populations contribute to T cell development to different extents. Fate-mapping experiments have shown that 85% of ETPs

display a history of *Il7r* expression, suggesting that the majority of thymocytes might be derived from CLPs, CLP-like cells, or late MPPs [27,50]. However, these findings might also be explained by preferential intrathymic expansion of this fraction of TSPs. Transfer experiments have shown that CLPs and MPPs progress developmentally with different kinetics once within the thymus [25,26,51]. Thus, CLPs already give rise to a substantial frequency of DP thymocytes after 7 days, showing faster differentiation kinetics compared with the average lifetime of ETPs. At the same time, CLPs generate one wave of T cell development that is complete after 4 weeks. By contrast, MPP-derived ETPs can be detected for at least 2 weeks resulting in a delayed appearance of DP cells. Notably, MPP-derived T cell development does not decline significantly until at least 4 weeks after transfer, suggesting the presence of long-lived progenitor cells within this subset. These findings are also consistent with the transient self-renewal potential of MPPs in BM [3,4]. It remains an open question for how long this property of MPPs is maintained after entry into the thymus. Interestingly, in the absence of competent TSPs thymus-autonomous T cell development is sustained for multiple months, demonstrating the substantial self-renewal capacity of intrathymic progenitors [52]. The reason for a two-tiered system of early T cell development remains unclear. However, given the periodicity of thymus colonization with its prolonged refractory intervals, the combination of immediate CLP-based and prolonged MPP-based T cell development might ensure continuous T cell output despite discontinuous input (Figure 2). Single-cell-based techniques are likely to foster our understanding of the interdependence of longevity, proliferation, and lineage commitment. Possibly, a refined version of the extant computational model will also help answer some of these questions [49,53].

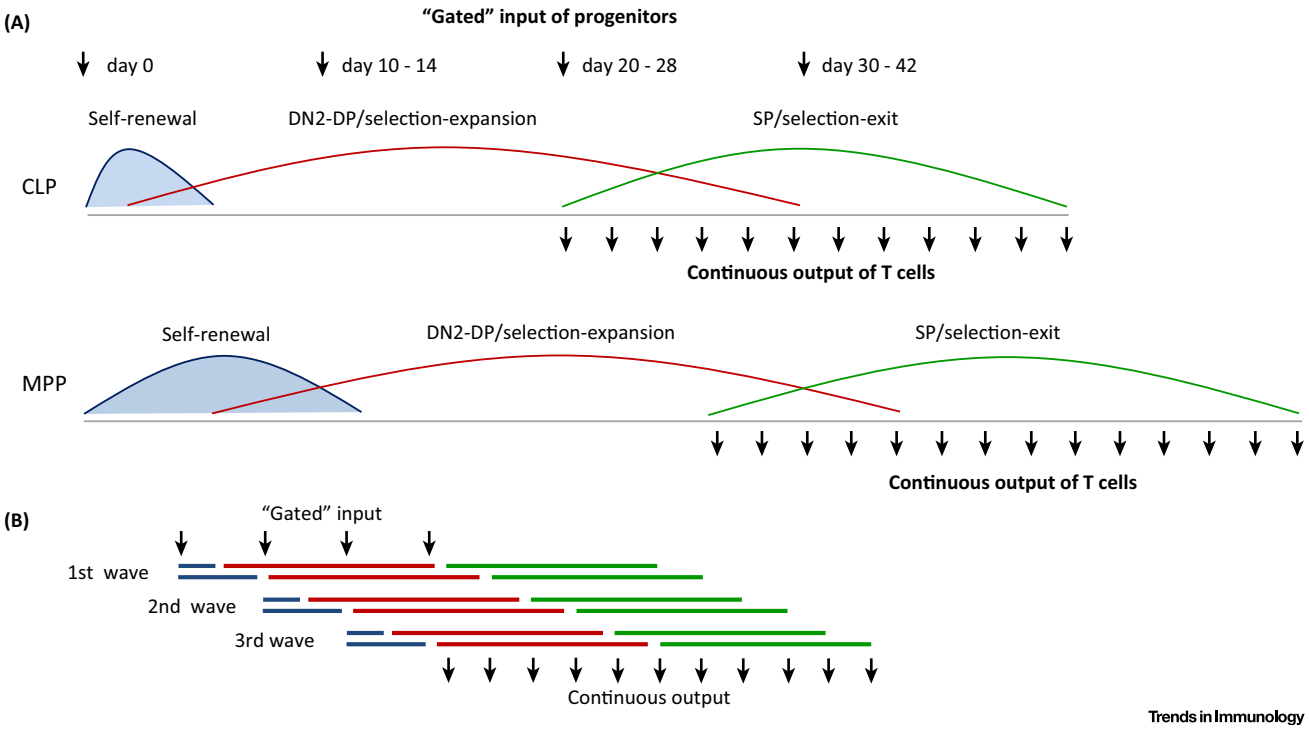

Figure 2. Gated Entry of Multiple Progenitors Generates a Continuous Output of Mature T Cells. (A) Two major populations of bone marrow-derived progenitors that contribute to T cell development – common lymphoid progenitors (CLPs) and multipotent progenitors (MPPs) – enter the thymus simultaneously in a 'gated' manner. Their differing self-renewal potentials and times of differentiation ensure continuous efflux of mature T cells into the periphery. (B) Multiple waves of progenitors that enter the thymus contribute to continuous export of mature T cells. DP, double positive; DN, double negative; SP, single positive.

T lineage commitment is completed as thymocytes transit through a short DN2 phase of 2–3 days before entering the DN3 stage, at which they start recombining the *Tcrb* locus (for αβT cells) and undergo the first selection checkpoint for productive TCR gene rearrangements. At the transition to this stage, massive expansion occurs resulting in 3×10^6 DN3s emerging from just 25 000 DN2s. The size of the DN3 compartment appears to be tightly regulated and remains almost constant even if cell numbers in more immature compartments are reduced. For instance, mice deficient in CCR7 and CCR9 display more than 100-fold reduction in numbers of ETPs and DN2s but only a twofold reduction in DN3s [28,32]. Other mouse models with transcription factor- or miRNA-mediated deficiency in ETPs, such as Tcf7-deficient mice and miR-17∼92-deficient mice, respectively, display a similar phenotype [54–56]. The mechanisms controlling the size of the DN3 compartment remain unknown. However, it can be speculated that size regulation is independent of output because Rag-deficient mice, in which all 'output' of this compartment is directed towards cell death, retain a normal-sized DN3 compartment. Furthermore, intrathymic redistribution does not affect DN3 numbers [57]. By contrast, deficiency in IL-7 signaling results in reduced overall thymocyte numbers including the DN3 compartment, suggesting that this pathway may contribute to the regulation of compartment size. Mathematical models analogous to those determining the flow through BM progenitor compartments might provide testable hypotheses on how the DN3 compartment is maintained [4].

Life-and-Death Decisions: From 100 000 000 to 10 000 000 in 3 Days

Thymocytes remain at the DN3 stage for about 4 days. On successful selection for expression of a productively rearranged TCRβ chain (i.e., β selection), cells transit through the highly proliferative DN4 or pre-DP stage and subsequently become DP thymocytes [58]. The average lifespan of DP thymocytes before selection was estimated to be in the range of 60 h, during which recombination of the *Tcra* locus occurs. This period is followed by a brief 16 h of positive selection and, in part, negative selection. Selection ultimately results in death of 90% of DP thymocytes [59–61].

Positive selection ensures the survival of cells expressing an αβTCR capable of recognizing peptide:MHC ligands. By contrast, negative selection results in clonal deletion of cells expressing a TCR recognizing self-antigen. Negative selection can occur simultaneously with positive selection in the thymic cortex, most likely leading to deletion of clones reactive to ubiquitously expressed self-antigens. Alternatively, positive selection induces migration to the thymic medulla, where thymocytes are probed for recognition of tissue-specific self-antigens, again resulting in deletion or terminal maturation and eventual egress from the thymus.

Attempts to quantify selection events yielded surprisingly contradictory results. Earlier studies were based on comparing thymocyte fate in MHC-deficient mice or on transfer into mice carrying cell type-specific MHC deficiency [62–64]. In combination, these studies remained inconclusive in that either the contribution of clonal deletion to overall thymocyte death was minute or deletion of MHC-responsive (i.e., positively selected) cells was between 5% and 65% depending on the assay system. Recently, a new approach to quantify thymocyte selection was undertaken using a combination of two mouse models: Bim-deficient mice, which have a defect in clonal deletion, and Nur77 reporter mice, in which reporter expression serves as an indicator of TCR signal strength [65]. Accordingly, in these mice increased numbers of thymocytes with high levels of reporter expression represent cells that would have undergone clonal deletion under wild-type conditions. Combining this system with calculations of the average lifespan of various thymocyte populations permitted the determination of thymic selection rates [60]. The overall estimate is that 5.5–6-times more cells undergo negative selection than complete positive selection. Among cells undergoing clonal deletion, 2–3-times more DP cells were deleted in the cortex compared with deletion of single-positive

(SP) cells in the medulla. To formally distinguish between death by neglect and clonal deletion, this study relied on a combination of CD5, CD69,and caspase 3 staining and established that approximately 25% of apoptosis in the thymus occurred due to negative selection [60]. Applying data from this study to a dynamical mathematical model has yielded somewhat discrepant results in suggesting that more than 90% of post-selection DP cells and, consequently, relatively few SP cells undergo clonal deletion [61]. Rates of 75% failure to undergo positive selection and clonal deletion predominantly occurring at the DP stage were also determined by applying a dynamical model to an experimental model of temporally inducible selection [66]. This study also showed that the ratio of two CD4 T cells developing for each CD8 T cell is due to cell death bias at the DP stage.

The murine thymus on average exports 1–4 $\times$ 10^6 $CD4^+$ and $CD8^+$ T cells per day, which is equivalent to 1% of all thymocytes [67,68]. Before newly selected SP thymocytes enter the long-lived T cell pool, they undergo a final step of maturation that starts in the thymus and continues for approximately 3 weeks in the periphery [69–72]. Molecular timers such as fluorescent reporter protein expression under the control of the Rag locus were instrumental in defining the post-selection residence time of thymocytes, which is in the range of 4 days [73]. Such experiments showed that egress from the thymus is not random but rather developmentally controlled and thus allowed molecular characterization of this process. Tonic type I IFN signaling and NF-κB kinase TAK1 were required for all aspects of functional maturation before egress [70]. These experiments highlight the potential of molecular timers at other stages of T cell development.

Concluding Remarks

Developing a good quantitative model of a biological process depends on the quality of data serving as input for computational models. Thus, some major progress has been made in recent years with the development of fate-mapping approaches, barcoding, and genetically encoded molecular timers. The most solid quantitative information on T cell development primarily exists at the level of the population dynamics of HSCs and their BM-resident descendants up to thymus colonization and then again for thymic selection (Figure 3 and Table 1). In between, early intrathymic T cell development characterized by commitment and vast proliferation remains quantitatively largely uncharted terrain. Furthermore, it remains to be established how age-dependent thymic involution and pretransplantation conditioning regimens affect intrathymic developmental dynamics, and computational models might provide surprising new insight. However, the biggest challenge in establishing quantitative models of T cell development remains its technical restriction to the mouse model. Obtaining comparable information for the human system cannot rely on sophisticated genetic tools and only rarely will it be possible to infer data directly from interventional regimens. Clonal dynamics of HSCs after gene therapy can be determined by mapping retroviral insertion sites as surrogate barcodes [74,75]. *In vitro* differentiation suggested that human progenitors generate T cells with slower kinetics than their murine counterparts [76]. One groundbreaking study directly compared age-dependent thymic output in human and mouse using TCR excision circles as molecular timers and *in vivo* cell labeling with deuterated water [77]. This study suggested that whereas in mice thymic output contributes to the majority of naïve T cells generated throughout life, in adult humans only 10–20% of naïve T cell production is thymus derived with the remainder being generated through homeostatic proliferation in the periphery. On an organismal level, humans and mice differ in lifespan by a factor of 30–50, size and total cellularity by a factor of 3000, and number of cell divisions throughout life by a factor of 10^5 [78]. Furthermore, murine cells have a higher basal metabolic rate and display profound differences in telomere biology, which directly affect the aging process [15,79]. It remains an open question whether these complex differences can be incorporated into computational models attempting to quantify human T cell development.

Outstanding Questions

Early steady-state and post-transplantation hematopoiesis have recently been shown to have fundamentally different dynamics. Is this also the case for intrathymic T cell development?

TSPs are a heterogeneous mixture of cells with distinct developmental and proliferative potentials. Can this heterogeneity be accurately captured by dynamic models to explain their flux through developmental stages?

How are the dynamics of T cell development quantitatively altered on age-dependent thymic involution?

Quantitation of T cell development depends on refined experimental setups predominantly based on genetically encoded reporters and has therefore been largely restricted to the mouse as a model organism. What experiments can best capture T cell developmental dynamics in the absence of (genetic) intervention? Are T cell developmental dynamics fundamentally different in mice and humans? If so, what are the underlying reasons?

What can we learn from computational models to improve T lineage regenerative therapies?

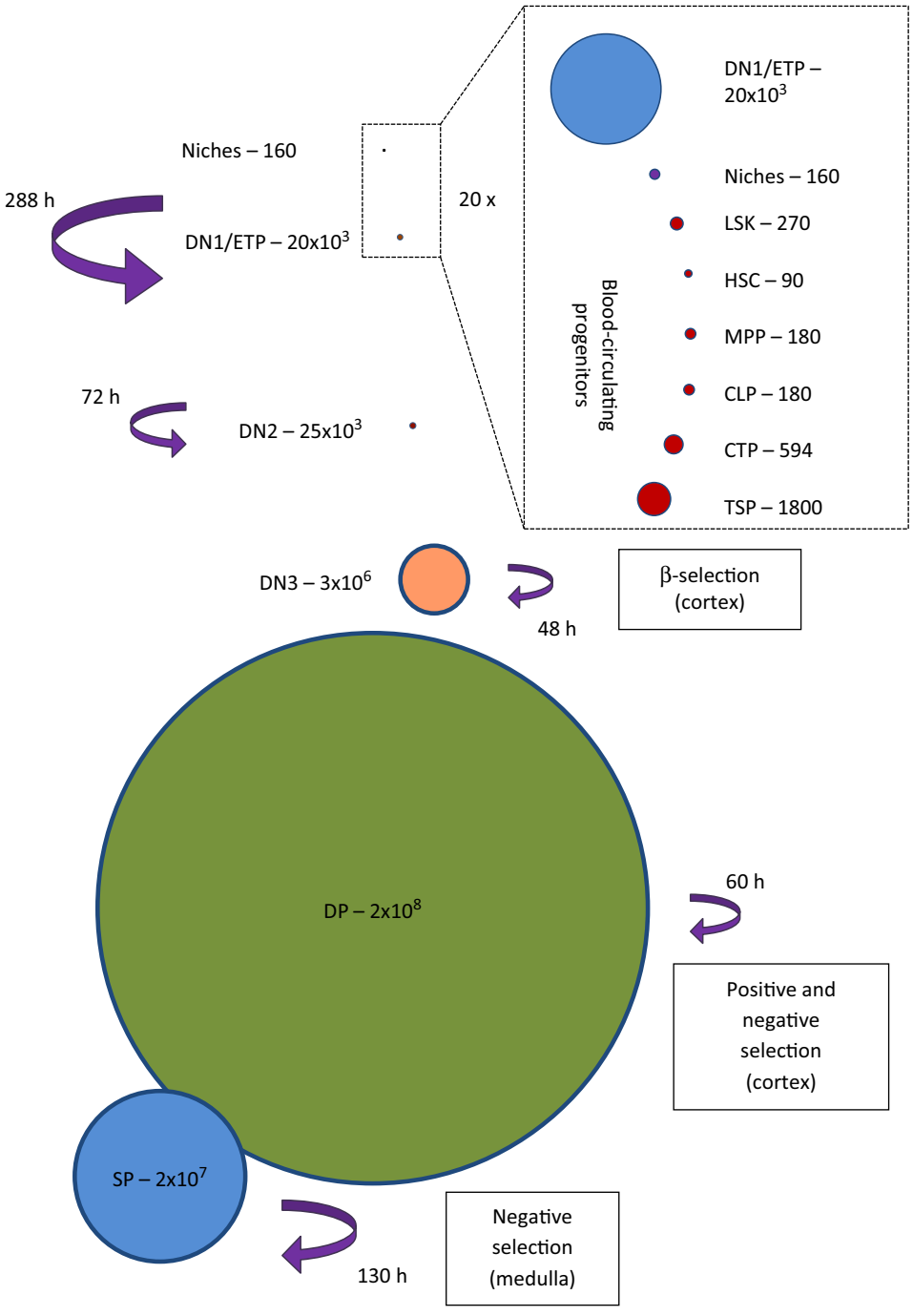

Figure 3. The Thymic Universe. Areas of circles and widths of arrows are proportional to the cellularity and lifespan of the indicated populations, respectively. TSP, thymus-seeding progenitor; LSK, $Lin^{-}Sca\text{-}1^{+}Kit^{+}$; HSC, hematopoietic stem cell; MPP, multipotent progenitor; CLP, common lymphoid progenitor; CTP, circulating T lineage-committed progenitor; DN, double negative; ETP, early T lineage progenitor; DP, double positive; SP, single positive.

Table 1. T Cell Development by the Numbers.

Population	Number	Residence time	Refs
BM[a]			
HSC	17×10^3	∞[b]	[4,14,80]
MPP	4.2×10^6	70 days	[4]
CLP	2.8×10^5	60 days	[4]
Blood[c]			
LSK	270	n.d.[d]	[18]
HSC	90	6 min	[18,24]
MPP	180	n.d.	[18,25,26]
CLP	180	n.d.	[25,26]
CTP	594	n.d.	[19]
TSP[e]	1800	n.d.	[25]
Thymus[f]			
TSP	160	60 h[g]	[38,49]
ETP	$2–3 \times 10^4$	216–288 h	[42,49]
DN2	$2–3 \times 10^4$	48–66 h	[42,49]
DN3	$2–3 \times 10^6$	48–96 h	[42,49,59]
DN3a	1.6×10^6	n.d.	[81]
DN3b	4×10^5	n.d.	[81]
DP	97×10^6	76 h	[60,61]
Pre-selection DP	88×10^6	60 h	[60,61]
Post-selection DP	8.5×10^6	16 h	[60,61]
SP	17×10^6	130 h	[60,61]
CD4 SP	12×10^6	130 h	[60,61]
CD8 SP	4×10^6	130 h	[60,61]
T regulatory	$5–8 \times 10^4$	130 h	[60,65]

[a]Based on 2.8×10^8 total nucleated cells [80].
[b]Rate of self-renewal: 1/110 to 1/10 per day.
[c]Estimated based on blood volume of 72 ml/kg body weight and 25 g body weight [82].
[d]Not determined.
[e]$Lin^-CD135^+CD27^+$.
[f]Based on $1–2 \times 10^8$ total thymocytes in 8–10-week-old mice.
[g]Time of occupancy of individual TSP niche: 9–11 days [38].

Acknowledgments

The authors dedicate this review to the memory of Dr Jacek Puchałka. They thank Immo Prinz for critical reading of the manuscript. Work in the laboratory of A.K. is funded by the German Research Foundation (DFG KR2320/3-1, KR2320/5-1, SFB738-A7, SFB902-B15).

References

1. Dudakov, J.A. and van den Brink, M.R. (2011) Greater than the sum of their parts: combination strategies for immune regeneration following allogeneic hematopoietic stem cell transplantation. *Best Pract. Res. Clin. Haematol.* 24, 467–476
2. Rothenberg, E.V. *et al.* (2016) Hematopoiesis and T-cell specification as a model developmental system. *Immunol. Rev.* 271, 72–97
3. Sun, J. *et al.* (2014) Clonal dynamics of native haematopoiesis. *Nature* 514, 322–327
4. Busch, K. *et al.* (2015) Fundamental properties of unperturbed haematopoiesis from stem cells *in vivo*. *Nature* 518, 542–546
5. Harrison, D.E. *et al.* (1988) Number and continuous proliferative pattern of transplanted primitive immunohematopoietic stem cells. *Proc. Natl. Acad. Sci. U. S. A.* 85, 822–826
6. Szilvassy, S.J. *et al.* (1990) Quantitative assay for totipotent reconstituting hematopoietic stem cells by a competitive repopulation strategy. *Proc. Natl. Acad. Sci. U. S. A.* 87, 8736–8740
7. Wilson, A. *et al.* (2008) Hematopoietic stem cells reversibly switch from dormancy to self-renewal during homeostasis and repair. *Cell* 135, 1118–1129

8. Lu, R. *et al.* (2011) Tracking single hematopoietic stem cells *in vivo* using high-throughput sequencing in conjunction with viral genetic barcoding. *Nat. Biotechnol.* 29, 928–933
9. Gerrits, A. *et al.* (2010) Cellular barcoding tool for clonal analysis in the hematopoietic system. *Blood* 115, 2610–2618
10. Naik, S.H. *et al.* (2013) Diverse and heritable lineage imprinting of early haematopoietic progenitors. *Nature* 496, 229–232
11. Perie, L. *et al.* (2014) Determining lineage pathways from cellular barcoding experiments. *Cell Rep.* 6, 617–624
12. Bystrykh, L.V. *et al.* (2012) Counting stem cells: methodological constraints. *Nat. Methods* 9, 567–574
13. Hofer, T. *et al.* (2016) Stem-cell dynamics and lineage topology from *in vivo* fate mapping in the hematopoietic system. *Curr. Opin. Biotechnol.* 39, 150–156
14. Sawai, C.M. *et al.* (2016) Hematopoietic stem cells are the major source of multilineage hematopoiesis in adult animals. *Immunity* 45, 597–609
15. Weber, T.S. *et al.* (2016) Site-specific recombinatorics: *in situ* cellular barcoding with the Cre Lox system. *BMC Syst. Biol.* 10, 43
16. Bhandoola, A. *et al.* (2007) Commitment and developmental potential of extrathymic and intrathymic T cell precursors: plenty to choose from. *Immunity* 26, 678–689
17. Schlenner, S.M. and Rodewald, H.R. (2010) Early T cell development and the pitfalls of potential. *Trends Immunol.* 31, 303–310
18. Schwarz, B.A. and Bhandoola, A. (2004) Circulating hematopoietic progenitors with T lineage potential. *Nat. Immunol.* 5, 953–960
19. Krueger, A. and von Boehmer, H. (2007) Identification of a T lineage-committed progenitor in adult blood. *Immunity* 26, 105–116
20. Umland, O. *et al.* (2007) The blood contains multiple distinct progenitor populations with clonogenic B and T lineage potential. *J. Immunol.* 178, 4147–4152
21. Lai, A.Y. and Kondo, M. (2007) Identification of a bone marrow precursor of the earliest thymocytes in adult mouse. *Proc. Natl. Acad. Sci. U. S. A.* 104, 6311–6316
22. Zlotoff, D.A. *et al.* (2008) The long road to the thymus: the generation, mobilization, and circulation of T-cell progenitors in mouse and man. *Semin. Immunopathol.* 30, 371–382
23. Goldschneider, I. (2006) Cyclical mobilization and gated importation of thymocyte progenitors in the adult mouse: evidence for a thymus-bone marrow feedback loop. *Immunol. Rev.* 209, 58–75
24. Wright, D.E. *et al.* (2001) Physiological migration of hematopoietic stem and progenitor cells. *Science* 294, 1933–1936
25. Serwold, T. *et al.* (2009) Reductive isolation from bone marrow and blood implicates common lymphoid progenitors as the major source of thymopoiesis. *Blood* 113, 807–815
26. Saran, N. *et al.* (2010) Multiple extrathymic precursors contribute to T-cell development with different kinetics. *Blood* 115, 1137–1144
27. Schlenner, S.M. *et al.* (2010) Fate mapping reveals separate origins of T cells and myeloid lineages in the thymus. *Immunity* 32, 426–436
28. Krueger, A. *et al.* (2010) CC chemokine receptor 7 and 9 double-deficient hematopoietic progenitors are severely impaired in seeding the adult thymus. *Blood* 115, 1906–1912
29. Svensson, M. *et al.* (2008) Involvement of CCR9 at multiple stages of adult T lymphopoiesis. *J. Leukoc. Biol.* 83, 156–164
30. Rossi, F.M. *et al.* (2005) Recruitment of adult thymic progenitors is regulated by P-selectin and its ligand PSGL-1. *Nat. Immunol.* 6, 626–634
31. Veerman, K.M. *et al.* (2007) Interaction of the selectin ligand PSGL-1 with chemokines CCL21 and CCL19 facilitates efficient homing of T cells to secondary lymphoid organs. *Nat. Immunol.* 8, 532–539
32. Zlotoff, D.A. *et al.* (2010) CCR7 and CCR9 together recruit hematopoietic progenitors to the adult thymus. *Blood* 115, 1897–1905
33. Scollay, R. *et al.* (1986) Dynamics of early T cells: prothymocyte migration and proliferation in the adult mouse thymus. *Immunol. Rev.* 91, 129–157
34. Wallis, V.J. *et al.* (1975) On the sparse seeding of bone marrow and thymus in radiation chimaeras. *Transplantation* 19, 2–11
35. Mori, S. *et al.* (2001) Characterization of thymus-seeding precursor cells from mouse bone marrow. *Blood* 98, 696–704
36. Scimone, M.L. *et al.* (2006) A multistep adhesion cascade for lymphoid progenitor cell homing to the thymus. *Proc. Natl. Acad. Sci. U. S. A.* 103, 7006–7011
37. Gossens, K. *et al.* (2009) Thymic progenitor homing and lymphocyte homeostasis are linked via S1P-controlled expression of thymic P-selectin/CCL25. *J. Exp. Med.* 206, 761–778
38. Zietara, N. *et al.* (2015) Multicongenic fate mapping quantification of dynamics of thymus colonization. *J. Exp. Med.* 212, 1589–1601
39. Foss, D.L. *et al.* (2001) The importation of hematogenous precursors by the thymus is a gated phenomenon in normal adult mice. *J. Exp. Med.* 193, 365–374
40. Foss, D.L. *et al.* (2002) Functional demonstration of intrathymic binding sites and microvascular gates for prothymocytes in irradiated mice. *Int. Immunol.* 14, 331–338
41. Lind, E.F. *et al.* (2001) Mapping precursor movement through the postnatal thymus reveals specific microenvironments supporting defined stages of early lymphoid development. *J. Exp. Med.* 194, 127–134
42. Porritt, H.E. *et al.* (2003) Kinetics of steady-state differentiation and mapping of intrathymic-signaling environments by stem cell transplantation in nonirradiated mice. *J. Exp. Med.* 198, 957–962
43. Lucas, B. *et al.* (2016) Lymphotoxin beta receptor controls T cell progenitor entry to the thymus. *J. Immunol.* 197, 2665–2672
44. Shi, Y. *et al.* (2016) LTβR controls thymic portal endothelial cells for haematopoietic progenitor cell homing and T-cell regeneration. *Nat. Commun.* 7, 12369
45. Buono, M. *et al.* (2016) A dynamic niche provides Kit ligand in a stage-specific manner to the earliest thymocyte progenitors. *Nat. Cell Biol.* 18, 157–167
46. Prockop, S.E. and Petrie, H.T. (2004) Regulation of thymus size by competition for stromal niches among early T cell progenitors. *J. Immunol.* 173, 1604–1611
47. Richie Ehrlich, L.I. *et al.* (2011) *In vitro* assays misrepresent *in vivo* lineage potentials of murine lymphoid progenitors. *Blood* 117, 2618–2624
48. Lyszkiewicz, M. *et al.* (2015) Limited niche availability suppresses murine intrathymic dendritic-cell development from noncommitted progenitors. *Blood* 125, 457–464
49. Manesso, E. *et al.* (2013) Computational modelling of T-cell formation kinetics: output regulated by initial proliferation-linked deferral of developmental competence. *J. R. Soc. Interface* 10, 20120774
50. Belyaev, N.N. *et al.* (2010) Induction of an IL7-R^{+}c-Kit^{hi} myelolymphoid progenitor critically dependent on IFN-γ signaling during acute malaria. *Nat. Immunol.* 11, 477–485
51. Schwarz, B.A. *et al.* (2007) Selective thymus settling regulated by cytokine and chemokine receptors. *J. Immunol.* 178, 2008–2017
52. Peaudecerf, L. *et al.* (2012) Thymocytes may persist and differentiate without any input from bone marrow progenitors. *J. Exp. Med.* 209, 1401–1408
53. Manesso, E. *et al.* (2013) Dynamical modelling of haematopoiesis: an integrated view over the system in homeostasis and under perturbation. *J. R. Soc. Interface* 10, 20120817
54. Germar, K. *et al.* (2011) T-cell factor 1 is a gatekeeper for T-cell specification in response to Notch signaling. *Proc. Natl. Acad. Sci. U. S. A.* 108, 20060–20065
55. Weber, B.N. *et al.* (2011) A critical role for TCF-1 in T-lineage specification and differentiation. *Nature* 476, 63–68
56. Regelin, M. *et al.* (2015) Responsiveness of developing T cells to IL-7 signals is sustained by miR-17~92. *J. Immunol.* 195, 4832–4840
57. Benz, C. *et al.* (2004) Homing of immature thymocytes to the subcapsular microenvironment within the thymus is not an absolute requirement for T cell development. *Eur. J. Immunol.* 34, 3652–3663
58. Stritesky, G.L. *et al.* (2012) Selection of self-reactive T cells in the thymus. *Annu. Rev. Immunol.* 30, 95–114

59. Egerton, M. *et al.* (1990) Kinetics of mature T-cell development in the thymus. *Proc. Natl. Acad. Sci. U. S. A.* 87, 2579–2582

60. Stritesky, G.L. *et al.* (2013) Murine thymic selection quantified using a unique method to capture deleted T cells. *Proc. Natl. Acad. Sci. U. S. A.* 110, 4679–4684

61. Sawicka, M. *et al.* (2014) From pre-DP, post-DP, SP4, and SP8 thymocyte cell counts to a dynamical model of cortical and medullary selection. *Front. Immunol.* 5, 19

62. Surh, C.D. and Sprent, J. (1994) T-cell apoptosis detected *in situ* during positive and negative selection in the thymus. *Nature* 372, 100–103

63. Laufer, T.M. *et al.* (1996) Unopposed positive selection and autoreactivity in mice expressing class II MHC only on thymic cortex. *Nature* 383, 81–85

64. van Meerwijk, J.P. *et al.* (1997) Quantitative impact of thymic clonal deletion on the T cell repertoire. *J. Exp. Med.* 185, 377–383

65. Moran, A.E. *et al.* (2011) T cell receptor signal strength in Treg and iNKT cell development demonstrated by a novel fluorescent reporter mouse. *J. Exp. Med.* 208, 1279–1289

66. Sinclair, C. *et al.* (2013) Asymmetric thymocyte death underlies the CD4:CD8 T-cell ratio in the adaptive immune system. *Proc. Natl. Acad. Sci. U. S. A.* 110, E2905–E2914

67. Scollay, R.G. *et al.* (1980) Thymus cell migration. Quantitative aspects of cellular traffic from the thymus to the periphery in mice. *Eur. J. Immunol.* 10, 210–218

68. Scollay, R. and Shortman, K. (1985) Identification of early stages of T lymphocyte development in the thymus cortex and medulla. *J. Immunol.* 134, 3632–3642

69. Hogquist, K.A. *et al.* (2015) T cell adolescence: maturation events beyond positive selection. *J. Immunol.* 195, 1351–1357

70. Xing, Y. *et al.* (2016) Late stages of T cell maturation in the thymus involve NF-κB and tonic type I interferon signaling. *Nat. Immunol.* 17, 565–573

71. Boursalian, T.E. *et al.* (2004) Continued maturation of thymic emigrants in the periphery. *Nat. Immunol.* 5, 418–425

72. Berkley, A.M. *et al.* (2013) Recent thymic emigrants and mature naive T cells exhibit differential DNA methylation at key cytokine loci. *J. Immunol.* 190, 6180–6186

73. McCaughtry, T.M. *et al.* (2007) Thymic emigration revisited. *J. Exp. Med.* 204, 2513–2520

74. Wang, G.P. *et al.* (2010) Dynamics of gene-modified progenitor cells analyzed by tracking retroviral integration sites in a human SCID-X1 gene therapy trial. *Blood* 115, 4356–4366

75. Aiuti, A. *et al.* (2007) Multilineage hematopoietic reconstitution without clonal selection in ADA-SCID patients treated with stem cell gene therapy. *J. Clin. Invest.* 117, 2233–2240

76. La Motte-Mohs, R.N. *et al.* (2005) Induction of T-cell development from human cord blood hematopoietic stem cells by Delta-like 1 *in vitro*. *Blood* 105, 1431–1439

77. den Braber, I. *et al.* (2012) Maintenance of peripheral naive T cells is sustained by thymus output in mice but not humans. *Immunity* 36, 288–297

78. Rangarajan, A. and Weinberg, R.A. (2003) Opinion: comparative biology of mouse versus human cells: modelling human cancer in mice. *Nat. Rev. Cancer* 3, 952–959

79. Calado, R.T. and Dumitriu, B. (2013) Telomere dynamics in mice and humans. *Semin. Hematol.* 50, 165–174

80. Boggs, D.R. (1984) The total marrow mass of the mouse: a simplified method of measurement. *Am. J. Hematol.* 16, 277–286

81. Visan, I. *et al.* (2010) Lunatic fringe enhances competition for Delta-like Notch ligands but does not overcome defective pre-TCR signaling during thymocyte β-selection *in vivo*. *J. Immunol.* 185, 4609–4617

82. Diehl, K.H. *et al.* (2001) A good practice guide to the administration of substances and removal of blood, including routes and volumes. *J. Appl. Toxicol.* 21, 15–23